Journal of Non-Newtonian Fluid Mechanics, 51 (1994) 161–178
Elsevier Science B.V.

Effects of surface viscosity on the finite deformation of a liquid drop and the rheology of dilute emulsions in simple shearing flow

C. Pozrikidis

Department of Applied Mechanics and Engineering Sciences, University of California at San Diego, La Jolla, CA 92093-0411 (USA)

(Received June 9, 1993; in revised form August 24, 1993)

Abstract

The deformation of a liquid drop with constant isotropic surface tension and finite surface viscosity, evolving under the action of a simple shearing flow, is considered. The evolution of the drop from the spherical shape is computed using a novel implementation of the boundary integral method that incorporates the effects of interfacial rheology in an efficient manner. The numerical results confirm that surface viscosity acts to suppress the interfacial motion and reduce the magnitude of drop deformation. When the surface viscosity is sufficiently large, the drops maintain a compact shape at all capillary numbers. The effect of surface viscosity on the rheology of a dilute emulsion is considered, and it is found that, in all cases, a dilute emulsion behaves like a shear-thinning medium with some elastic properties.

Keywords: boundary integral method; dilute emulsions; liquid drop; simple shear flow; surface viscosity

1. Introduction

Boussinesq [1] noted that, due to the presence of impurities and surface active agents, the surface of a drop behaves like a distinct two-dimensional medium whose mechanical properties are more involved than those expressed by an isotropic surface tension. Furthermore, he recognized that interfacial rheology acts to modify the terminal velocity of a settling drop from the standard value computed by Hadamard and Rybczynski for a spherical drop with isotropic surface tension. Assuming that the drop interface exhibits viscous characteristics with shear surface viscosity ϵ,

SSDI 0377-0257(93)01195-A

Boussinesq found that the terminal velocity may still be computed from the formula of Hadamard and Rybczynski, provided that the viscosity of the drop is increased by an amount that is proportional to the surface viscosity ϵ.

Much later, Oldroyd [2] noted that the surface viscosity plays an important role in determining the effective viscosity of an emulsion, and derived expressions for the effective shear viscosity of a dilute suspension of spherical drops in terms of the dilatational viscosity κ and shear viscosity ϵ of the drop interface (see Appendix of this paper).

The values of the coefficients κ and ϵ depend, among other factors, on the chemical composition of the interface and on the temperature, and are not easy to measure. Wei et al. [3] proposed that, since the flow around and inside a drop is affected by ϵ and κ, observations of the flow about a drop in a definable field of flow may be used to deduce particular combinations of the values of ϵ and κ. Specifically, they proposed deducing the combination $3\kappa + 2\epsilon$ from the period of rotation of tracers at the mid-plane of a spherical drop that is immersed in a simple shearing flow. Wei et al. [3] applied their theoretical predictions to available experimental data, but the success of their conclusions could not be assessed.

The analyses of Boussinesq [1], Oldroyd [2] and Wei et al. [3] pertain to drops with either high surface tension, or high drop viscosity, or high surface viscosity, which are necessary in order for the drop to maintain the spherical shape. When these conditions are not met, the drops are significantly deformed, with the nature and magnitude of deformation depending upon the type and intensity of the incident flow.

The effect of surface viscosity and of variations in surface tension on the small deformation and orientation of nearly spherical drops was considered by Flumerfelt [4], and accompanying experiments were conducted by Phillips et al. [5]. One important finding is that, for small deformations, the effect of small variations in surface tension may be incorporated into an effective surface viscosity. The results of Flumerfelt provide a basis for the computation of ϵ and κ in terms of observations of the drop deformation and orientation in a simple shearing flow. In a related study, Barthes-Biesel and Sgaier [6] studied the transient deformation of a spherical drop with a viscoelastic interface. Since their objective was to describe the deformation of capsules and red blood cells, their analysis focused on elastic effects and did not incorporate the presence of isotropic surface tension.

One common conclusion of the analyses discussed above is that increasing the surface viscosity acts to increase effectively the viscosity of the drop by some factor. A physical explanation is that high surface viscosity suppresses the interfacial flow and makes the drop behave like a rigid particle, which may be considered a liquid drop with infinite viscosity. This

observation implies that increasing the surface viscosity will have the same qualitative effect as increasing the drop viscosity. It is known, for instance, that in the absence of surface viscosity, there is a critical ratio between the viscosity of the drop and the viscosity of the ambient fluid, λ_{cr}, above which a drop that is immersed in a simple shearing flow deforms and reaches a stationary shape independently of the value of surface tension. Below this critical value the drop exhibits large deformations and breaks up when the surface tension is sufficiently low. We expect then that, as the surface viscosity is increased, the value of λ_{cr} will diminish, which suggests that drop deformation may be reduced by increasing either the surface tension, or the surface viscosity, or the drop viscosity. The precise effect of surface viscosity on finite drop deformation and on the rheology of dilute emulsions has not been considered.

In this paper we develop a numerical method for computing the three-dimensional motion of a drop with constant surface tension and finite surface viscosity suspended in a Stokes flow. The numerical method is without intrinsic limitations as far as describing large deformations and handling arbitrary fluid and surface viscosities, but we find that high computational cost and numerical instabilities restrict its usefulness to cases of moderate deformations and drops with viscosity equal to that of the ambient fluid, $\lambda = 1$. Furthermore, it is assumed that the values of all γ, ϵ, and κ are constant. In reality, the values of all these parameters will depend upon the local temperature and chemical composition of the interface, factors which are absent from the mathematical formulation [7].

The numerical method is applied to study the effect of surface viscosity on the behaviour of moderately deformed drops in a suddenly applied simple shearing flow, including effects on the rheology of dilute emulsions. To the author's knowledge, this is the first attempt to describe finite three-dimensional deformations in the presence of interfacial rheology. The numerical results extend previous asymptotic analyses for drops with spherical and slightly deformed shapes discussed above. Furthermore, the present study extends previous research on the deformation of drops with constant surface tension and vanishing surface viscosity, and associated rheology of dilute emulsions. The latter was studied on a number of occasions using asymptotic and numerical methods. A recent contribution is the numerical investigation of Kennedy et al. [8] which is based on an advanced implementation of the boundary integral method. The reader is referred to that paper for an extensive discussion of the literature and further references.

To this end, it is appropriate to place the presently adopted model for interfacial rheology into the more general context of interfacial dynamics and discuss its physical relevance. As mentioned above, we consider drops with inertia-free interfaces that behave like two-dimensional Newtonian

fluids with constant surface tension and constant dilatational and shear surface viscosities. This formulation of interfacial rheology stems from the works of Boussinesq [1] and Scriven [9] who regard a fluid interface as a distinct medium with its own physico-chemical constants. Scriven develops Newtonian constitutive equations involving an isotropic surface tension γ, which is analogous to the pressure in an inviscid fluid, and dilatational and shear viscosities ϵ and κ. His model is expected to apply to pure or slightly contaminated interfaces with simple chemistry but, evidently, it is not adequate for describing the dynamics of more complex interfaces with some intrinsic structure. An example of the latter is the interface of a red blood cell which is composed of a lipid bi-layer that rests on a proteinic network. The red blood cell membrane is known to exhibit incompressible and viscoelastic characteristics.

It should also be emphasized that the applicability of the Newtonian surface model to drops whose interface exhibits large variations in surfactant concentration is not established. A better way of computing drop deformations in those cases would be to solve the convection–diffusion equation for the surfactant concentration and then introduce a constitutive equation for the interfacial stresses in terms of the surfactant concentration, thereby coupling the interfacial flow with the bulk flow. This procedure was implemented by Stone and Leal [10] and Milliken et al. [11] using a combination of boundary integral and finite-difference methods for the case of axisymmetric deformations of drops in a uniaxial straining flow in the presence of insoluble surfactants. In the case of the three-dimensional deformations presently considered, however, solving for the distribution of surfactants presents considerable computational challenges.

2. Problem statement and formulation

We consider the transient deformation of a spherical drop with viscosity $\lambda\mu$ suspended in an infinite fluid with viscosity μ, subject to an incident simple shearing flow $\boldsymbol{u}^{\infty} = (ky, 0, 0)$, as illustrated in Fig. 1.

To describe the motion of the drop interface we introduce two surface coordinates ξ and η, cover the interface with a grid of size N by M, and compute the motion of marker points that are identified by the intersections of successive grid lines. At the initial instant, ξ lines are lines of constant z, and η lines are lines of constant meridional angle θ. For computational convenience, we stipulate that the marker points are topological beacons, that is, they move with the velocity of the fluid normal to the interface, i.e.

$$\frac{\mathrm{d}\boldsymbol{X}}{\mathrm{d}t}(\xi, \eta, t) = \boldsymbol{u}(\xi, \eta, t) \cdot \boldsymbol{n}(\xi, \eta, t). \tag{1}$$

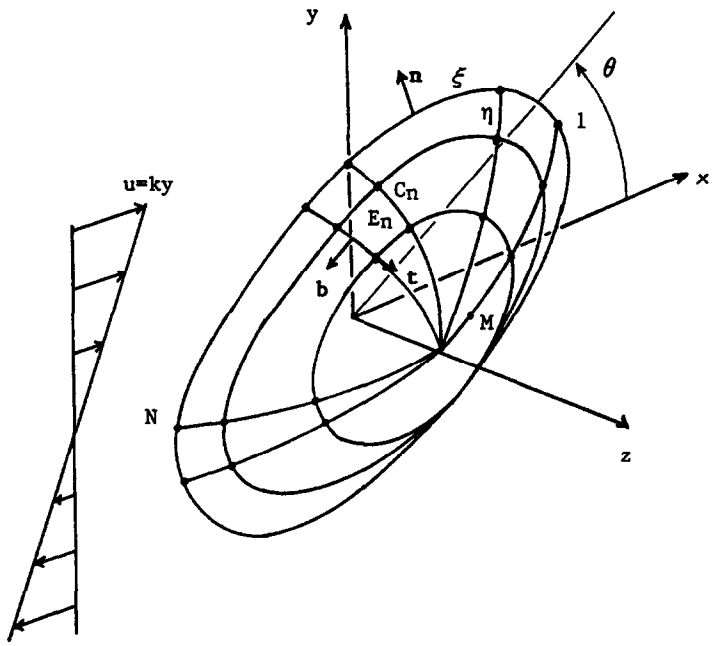

Fig. 1. Schematic illustration of a drop in a simple shear flow showing the system of surface coordinates.

Here $\boldsymbol{X}$ signifies the position of a marker point, and $\boldsymbol{n}$ is the unit vector normal to the interface pointing into the ambient fluid (Fig. 1).

At small Reynolds numbers, the fluid flow inside the outside the drop is governed by the equations of creeping flow, including the Stokes equation and the continuity equation [12]. The internal and external flows match through a kinematic boundary condition which requires that the velocity is continuous across the interface, and a dynamic boundary condition which requires that the discontinuity in hydrodynamic traction across the interface, $\Delta \boldsymbol{f} = [\sigma^{(\text{External})} - \sigma^{(\text{Internal})}] \cdot \boldsymbol{n}$, is balanced by the surface stress tensor. The latter is assumed to act in the plane of the interface; its precise form depends upon the rheological properties of the interface.

The interface of the drop is assumed to have a constant isotropic tension γ and to exhibit Newtonian characteristics. Scriven [9] provides a constitutive equation for the rheology of a Newtonian interface in surface curvilinear coordinates. Secomb and Skalak [13] note that, in order to obtain a unified description of the bulk flow on either side of the interface and of the surface flow in the plane of the interface, it is preferable to work in global Cartesian coordinates. Thus, they introduce the Cartesian surface-rate-of-strain tensor $\boldsymbol{e}^{(s)}$ and corresponding surface-viscous-stress tensor $\boldsymbol{\sigma}^{(s)}$, and their smooth but arbitrary extensions off the plane of the interface, and

rewrite the constitutive equation for a Newtonian interface in Cartesian coordinates as

$$\sigma_{ij}^{(s)} = \gamma P_{ij} + (\kappa - \epsilon)\theta P_{ij} + 2\epsilon e_{ij}^{(s)}, \tag{2}$$

where the superscript (s) signifies "surface". Here ϵ is the surface shear viscosity, κ is the surface dilatational viscosity, θ is the rate-of-dilatation of the interface, and $\boldsymbol{P}$ is the surface projection tensor defined as $P_{ij} = \delta_{ij} - n_i n_j$ where δ_{ij} is Kronecker's delta. Furthermore, Secomb and Skalak [13] show that $\boldsymbol{e}^{(s)}$ and θ may be computed from the velocity field as

$$e_{ij}^{(s)} = \tfrac{1}{2} P_{ik} P_{jl} \left(\frac{\partial u_k}{\partial x_l} + \frac{\partial u_l}{\partial x_k} \right), \qquad \theta = P_{ij} \frac{\partial u_i}{\partial x_j}. \tag{3}$$

It is important to note that the projection operator in (3) removes derivatives of the velocity in a direction normal to the interface, as well as derivatives of the velocity component normal to the interface in a direction tangential to the interface. Thus, $\boldsymbol{e}^{(s)}$ and θ may be computed from knowledge of the velocity in the plane of the interface alone.

The shape of a drop and associated velocity field may be used to compute the effective stress tensor $\langle \boldsymbol{\sigma} \rangle$ of a dilute emulsion of drops in a simple shear flow. Following Refs. 8 and 14 we find

$$\langle \sigma_{ij} \rangle = -\delta_{ij} \langle P \rangle + 2\mu \langle e_{ij} \rangle + m \int_S [\Delta f_i x_j - \mu(1-\lambda)(u_i n_j + u_j n_i)] \, \mathrm{d}S, \tag{4}$$

where $\langle\ \rangle$ signifies volume average values, and m is the number of drops per unit volume in the suspension. The last integral on the right-hand side of (4) is known as the *stresslet* or *particle stress tensor*, and will be denoted by Σ.

The viscosity of the drop interface is responsible for dissipating a certain amount of energy that contributes to the effective shear stress of an emulsion. Secomb and Skalak [13] show that the rate of viscous dissipation within the interface is given by

$$D^{(s)} = \int_S \{\kappa\theta^2 + 2\epsilon[\boldsymbol{e}^{(s)} - \tfrac{1}{2}\theta \boldsymbol{P}] : [\boldsymbol{e}^{(s)} - \tfrac{1}{2}\theta \boldsymbol{P}]\} \, \mathrm{d}S. \tag{5}$$

2.1 Boundary integral formulation

To obtain the instantaneous velocity field, we use the boundary integral method for Stokes flow [12, Chapter 5]. Following a standard procedure we obtain the following integral equation for the interfacial velocity:

$$u_j(\boldsymbol{x}_0) = \frac{2}{1+\lambda} u_j^{\infty}(\boldsymbol{x}_0) - \frac{1}{4\pi\mu} \frac{1}{\lambda+1} \int_S \Delta f_i(\boldsymbol{x}) G_{ij}(\boldsymbol{x}, \boldsymbol{x}_0) \, \mathrm{d}S(\boldsymbol{x}) + \frac{\beta}{4\pi} \int_S^{PV} u_i(\boldsymbol{x}) T_{ijk}(\boldsymbol{x}, \boldsymbol{x}_0) n_k(\boldsymbol{x}) \, \mathrm{d}S(\boldsymbol{x}), \tag{6}$$

where the point $\boldsymbol{x}_0$ is assumed to be on the interface, and PV designates the Principal Value of the improper integral. Also, $\beta = (\lambda - 1)/(\lambda + 1)$, $\Delta \boldsymbol{f}$ is the discontinuity in the surface force across the interface defined above, and

$$G_{ij}(\boldsymbol{x}, \boldsymbol{x}_0) = \frac{\delta_{ij}}{\|\hat{\boldsymbol{x}}\|} + \frac{\hat{x}_i \hat{x}_j}{\|\hat{\boldsymbol{x}}\|^3} \qquad T_{ijk}(\boldsymbol{x}, \boldsymbol{x}_0) = -6\frac{\hat{x}_i \hat{x}_j \hat{x}_k}{\|\hat{\boldsymbol{x}}\|^5}, \quad \text{with } \hat{\boldsymbol{x}} = \boldsymbol{x} - \boldsymbol{x}_0 \quad (7)$$

are, respectively, the free-space Green's functions for the velocity and stress. The first integral on the right-hand side of (6) is called the single-layer integral, and the second integral is called the double-layer integral.

The value of $\Delta \boldsymbol{f}$ depends upon the distribution of the surface stress tensor $\boldsymbol{\sigma}^{(s)}$ over the interface. Given $\Delta \boldsymbol{f}$, we solve (6) for the interfacial velocity, and then advance the position of the marker points according to eqn. (1).

It is important to note that the interfacial velocity appears in three places in eqn. (6): (i) explicitly on the left-hand side, (ii) implicitly within the surface stress tensor which is used to define $\Delta \boldsymbol{f}$, and (iii) explicitly within the principal value of the double-layer integral. When the surface viscosities κ and ϵ vanish, the second contribution disappears and (6) becomes a Fredholm integral equation of the second kind for the interfacial velocity. In that case, a rigorous theoretical analysis shows that the equation may be solved by the method of successive substitutions for any value of the viscosity ratio λ [13]. This method involves guessing the interfacial velocity field, computing the surface stress tensor and substituting the result back into the right-hand side of (6), and finally replacing the original with the computed velocity. The procedure is repeated until convergence is achieved.

Unfortunately, a theoretical analysis of the general form of (6), maintaining the effect of surface viscosity, could not be performed, but exploratory computations using a variant of the numerical method described in Section 3 have shown that the method of successive substitutions converges only for small values of the ratios ϵ/μ and κ/μ, roughly smaller than 0.5. Unfortunately, this range is too narrow to render the iterative method useful in practice. As a compromise, we develop a direct method of solution which, however, has the crucial drawback of requiring a high computational cost.

3. Numerical method

One major task of the numerical method is the computation of the traction discontinuity across the interface, $\Delta \boldsymbol{f}$. This presents important challenges associated with the computation of the surface curvature tensor in terms of surface curvilinear coordinates, which erodes the accuracy of the numerical method [7]. To circumvent this problem, we replace the single-layer integral on the right-hand side of (6) with a sum of integrals over all

boundary elements E_n, and adopt a special form of the trapezoidal rule to write

$$\int_{E_n} \Delta f_i(\boldsymbol{x}) G_{ij}(\boldsymbol{x}, \boldsymbol{x}_0)\, \mathrm{d}S(\boldsymbol{x}) \approx \langle \Delta f_i \rangle_n \int_{E_n} G_{ij}(\boldsymbol{x}, \boldsymbol{x}_0)\, \mathrm{d}S(\boldsymbol{x}), \tag{8}$$

where

$$\langle \Delta f_i \rangle_n = \frac{1}{S_n} \int_{E_n} \Delta f_i(\boldsymbol{x})\, \mathrm{d}S(\boldsymbol{x}) \tag{9}$$

is the mean value of the discontinuity in the interfacial surface force over the element, and S_n is the surface area of the nth boundary element. Note that the boundary elements are defined in terms of the intersections of successive surface coordinate lines as shown in Fig. 1. The approximation shown in (8) was used previously by Pozrikidis [15] to compute the evolution of drops with constant surface tension in a three-dimensional lattice.

Requiring that the discontinuity in the surface force $\Delta \boldsymbol{f}$ balances the forces due to the surface stress tensor, we write the following force balance over an element:

$$\langle \Delta f_i \rangle_n = \frac{-1}{S_n} \int_{C_n} \sigma^{(s)}_{ik}(\boldsymbol{x}) b_k(\boldsymbol{x})\, \mathrm{d}l(\boldsymbol{x}), \tag{10}$$

where C_n is the contour of the element E_n, $\boldsymbol{b} = \boldsymbol{t} \times \boldsymbol{n}$, and $\boldsymbol{t}$ is the unit vector tangential to C_n taken in the counter-clockwise sense (Fig. 1). Substituting (10) into (8) and then into (6) we obtain the following approximate discrete integral equation

$$u_j(\boldsymbol{x}_0) \approx \frac{2}{1+\lambda} u_j^{\infty}(\boldsymbol{x}_0) + \frac{1}{4\pi\mu} \frac{1}{\lambda+1} \sum_{n=1}^{N} \frac{1}{S_n} \int_{C_n} \sigma^{(s)}_{ik}(\boldsymbol{x}) b_k(\boldsymbol{x})\, \mathrm{d}l(\boldsymbol{x}) \times \int_{E_n} G_{ij}(\boldsymbol{x}, \boldsymbol{x}_0)\, \mathrm{d}S(\boldsymbol{x}) + \frac{\beta}{4\pi} \int_S^{PV} u_i(\boldsymbol{x}) T_{ijk}(\boldsymbol{x}, \boldsymbol{x}_0) n_k(\boldsymbol{x})\, \mathrm{d}S(\boldsymbol{x}). \tag{11}$$

The next task is the computation of the surface stress tensor. According to (3), this requires computing derivatives of the Cartesian components of the interfacial velocity with respect to x, y, and z. In the numerical procedure, these derivatives are computed from the corresponding derivatives with respect to the surface coordinates ξ and η, as well as derivatives in the normal direction ζ. Specifically, using the chain rule, we find

$$\frac{\partial u_i}{\partial \xi} = \frac{\partial u_i}{\partial x_j} \frac{\partial x_j}{\partial \xi} \qquad \frac{\partial u_i}{\partial \eta} = \frac{\partial u_i}{\partial x_j} \frac{\partial x_j}{\partial \eta} \qquad \frac{\partial u_i}{\partial \zeta} = \frac{\partial u_i}{\partial x_j} \frac{\partial x_j}{\partial \zeta}, \tag{12}$$

which provides us with three linear systems of equations for $\partial u_i / \partial x_j$. The derivatives $\partial \boldsymbol{x} / \partial \xi$, $\partial \boldsymbol{x} / \partial \eta$ represent vectors that are tangential to the interface

along the ξ and η axes respectively, and are computed from knowledge of the instantaneous grid shape using centred differences. The derivatives $\partial \boldsymbol{u}/\partial\xi$, $\partial \mathbf{u}/\partial\eta$ are computed in a similar manner from the instantaneous interfacial velocity. For the purpose of computing $\boldsymbol{e}^{(s)}$ and θ using eqns. (3), the derivative $\partial \boldsymbol{x}/\partial\zeta$ is replaced by the normal vector $\boldsymbol{n}$, whereas the derivative $\partial \boldsymbol{u}/\partial\zeta$ is assigned an arbitrary value, physically representing an arbitrary extension of the velocity gradient tensor off the plane of the interface. The computed values of $\boldsymbol{e}^{(s)}$ and θ were confirmed to be independent of the arbitrarily assigned value of $\partial \boldsymbol{u}/\partial\zeta$.

The integrals over the contours of the boundary elements on the right-hand side of (11) are computed by applying the one-step trapezoidal rule, which yields the value of the integral from the values of the surface stress tensor and of the vector $\boldsymbol{b}$ at the grid points.

The main computational task is the solution of the integral equation (11). As mentioned in Section 2, we considered the feasibility of computing the solution using the method of successive substitutions, but could not achieve satisfactory convergence. As an alternative, we developed a direct method of solution. First, we rearrange (11) to obtain

$$\sum_{n=1}^{N} \frac{1}{S_n} \int_{C_n} \sigma_{ik}^{(s,v)}(\boldsymbol{x}) b_k(\boldsymbol{x})\, \mathrm{d}l(\boldsymbol{x}) \int_{E_n} G_{ij}(\boldsymbol{x}, \boldsymbol{x}_0)\, \mathrm{d}S(\boldsymbol{x}) + \mu(\lambda - 1) \int_S^{PV} u_i(\boldsymbol{x}) T_{ijk}(\boldsymbol{x}, \boldsymbol{x}_0) n_k(\boldsymbol{x})\, \mathrm{d}S(\boldsymbol{x}) - 8\pi\mu u_j(\boldsymbol{x}_0)$$
$$= -8\pi\mu u_j^{\infty}(\boldsymbol{x}_0) + \gamma \sum_{n=1}^{N} \frac{1}{S_n} \int_{C_n} b_i(\boldsymbol{x})\, \mathrm{d}l(\boldsymbol{x}) \int_{E_n} G_{ij}(\boldsymbol{x}, \boldsymbol{x}_0)\, \mathrm{d}S(\boldsymbol{x}), \tag{13}$$

where $\boldsymbol{\sigma}^{(s,v)}$ is the viscous part of the surface stress tensor containing the last two terms on the right-hand side of eqn. (2). It is important to note that the left-hand side of (13) is a linear function of the interfacial velocity, whereas the right-hand side is independent of the interfacial velocity.

In the numerical method, we apply (13) at all grid points and implement the numerical approximations described above to derive a system of linear equations for the interfacial velocity at the grid points, in the form

$$\sum_{m=1}^{L} A_{jim}(\boldsymbol{x}_k) u_i(\boldsymbol{x}_m) = B_j(\boldsymbol{x}_k), \tag{14}$$

where $k = 1, \ldots, L$, L is the total number of grid points, and summation is implied only over the index i. $\boldsymbol{B}$ stands for the right-hand side of (13). The coefficients A_{ijm} are computed by numerical differentiation by setting

$$A_{jim}(\boldsymbol{x}_k) = F_j[\text{at } \boldsymbol{x}_k, \text{ with } \boldsymbol{u}(\boldsymbol{x}_k) = 0 \text{ for all } k = 1, \ldots L, \text{ except } u_i(\boldsymbol{x}_m) = 1.0], \tag{15}$$

where $\boldsymbol{F}$ stands for the left-hand side of (13). The system (14) is solved using Gauss elimination. Having obtained the interfacial velocity, we advance the position of the grid points using Euler's method according to eqn. (1).

One important detail of the numerical method is that when (13) is applied at the solitary grid point at the $M+1$ ξ line lying on the z axis (Fig. 1), the accuracy worsens due to the singular nature of the grid. To circumvent this difficulty, we compute the velocity at the point by applying quadratic interpolation from the average values of the velocity over the Mth and $M-1$ ξ-level lines. Furthermore, exploiting the symmetries of the shear flow, we compute the velocity only over one quarter of the surface of the drop.

We found that the computations require a considerable amount of computational time. For instance, for the simplest case $\lambda = 1$ for which $\beta = 0$, and for a grid of size $N = 16$ and $M = 8$, each velocity calculation requires approximately 3 min of CPU time on the CRAY Y-MP computer of the San Diego Supercomputer Center. The total expense for one case study is close to 2 h and 30 min. For unequal viscosities, $\lambda \neq 1$ and a non-zero value of β, a single time step requires approximately 45 min of CPU time, which is clearly unacceptable. The vast majority of the computational effort was expended towards computing the influence matrix $\boldsymbol{A}$ in eqn. (14). These limitations force us to restrict our attention to the convenient case $\lambda = 1$.

The size of the time step is an important parameter of the numerical procedure. In agreement with previous experience, we found that the size of the time step must be kept below a threshold level in order to prevent the onset of numerical instabilities associated with the isotropic surface tension. At high values of the surface viscosity, we detected a saw-tooth numerical instability which is manifested as the drops approach a stationary shape. The onset of this instability could be delayed by decreasing the size of the time step, but could not be effectively screened out without resorting to numerical smoothing. Smoothing, however, was found to have a noticeable effect on the asymptotic drop deformation and was considered unacceptable (Section 4). Whether the viscous instability is due to the particular implementation of the numerical method, or is a manifestation of a more general behaviour, could not be assessed with confidence due to the high cost of the computations that prevented extensive experimentation.

In the course of a computation, the volume of the drop changed by a small amount due to numerical error. To suppress the accumulation of this error, we subjected the drop to an isotropic expansion or contraction at the end of each time step. The particle stress tensor $\boldsymbol{\Sigma}$ was computed using a discrete method that is analogous to that shown in eqn. (8).

4. Results and discussion

Non-dimensionalizing all variables using as a length scale the equivalent drop radius a, time scale the inverse shear rate of the incident flow $1/k$, velocity ak, and stress scale μk, we find that the behaviour of a drop depends on four non-dimensional parameters: the three viscosity ratios λ, $E = \epsilon/(a\mu)$, and $K = \kappa/(a\mu)$; and the Capillary number $Ca = \mu ak/\gamma$.

In our investigations we set $\lambda = 1$ in order to reduce the cost of the computations, and $E = K$ in order to reduce the available parametric space. We thus consider the motion in terms of the values of Ca and E.

The behaviour of drops with inviscid interfaces, $E = K = 0$, is well known [8]. Previous computations have shown that when $\lambda = 1$, a spherical drop deforms and obtains a stationary shape provided that Ca is approximately less than 0.37. At larger values of Ca the drop continues to elongate, becomes slender, and eventually breaks up.

To illustrate the effect of surface viscosity, in Fig. 2(a) we plot the history of drop deformation $D = (L - B)/(L + B)$ for $Ca = 0.10$ and several values of E. Here L is the maximum drop dimension and B is the minimum drop dimension in the xy plane. The computations terminate at that point in time where the numerical method becomes unstable. In Fig. 2(a), with straight horizontal lines, we also show the predictions of the small-deformation theory of Flumerfelt [4] for the steady deformations at large times (see Appendix). It is evident that the numerical results are consistent with the asymptotic predictions: increasing the surface viscosity makes the drop behave more like a rigid particle and decreases the drop deformation. The asymptotic values suggested by the computations are somewhat larger than those predicted by the small deformation theory. This tendency was also observed previously for drops with inviscid interfaces [8].

In Fig. 2(b) we plot the history of the drop orientation angle θ in the xy plane, defined in Fig. 1. In all cases, the drops begin to elongate along the principal direction of the rate of strain of the shear flow, which is a 45° angle, and then incline towards the x axis. Unfortunately, the approach to the steady orientation is slow, and it is difficult to extract the asymptotic values with reasonable accuracy at large and moderate values of E. Nevertheless, there is sufficient evidence to indicate serious disagreements between the numerical results and the predictions of the small deformation theory of Flumerfelt [4] represented by the straight horizontal lines (see Appendix). Similar discrepancies were reported for drops with $E = 0$ in Ref. 8.

In Fig. 2(c) we plot the evolution of the shearing component of the particle stress tensor which, under our non-dimensionalization, may be regarded as the effective shear viscosity of a dilute emulsion. Here and in the following discussion, the particle stress tensor is reduced with respect to the

value of its shearing component for a spherical drop with vanishing surface viscosity provided by Taylor [16]. This reduced particle stress tensor will be denoted by S. At the initial instant, when $E = 0$, the particle stress tensor

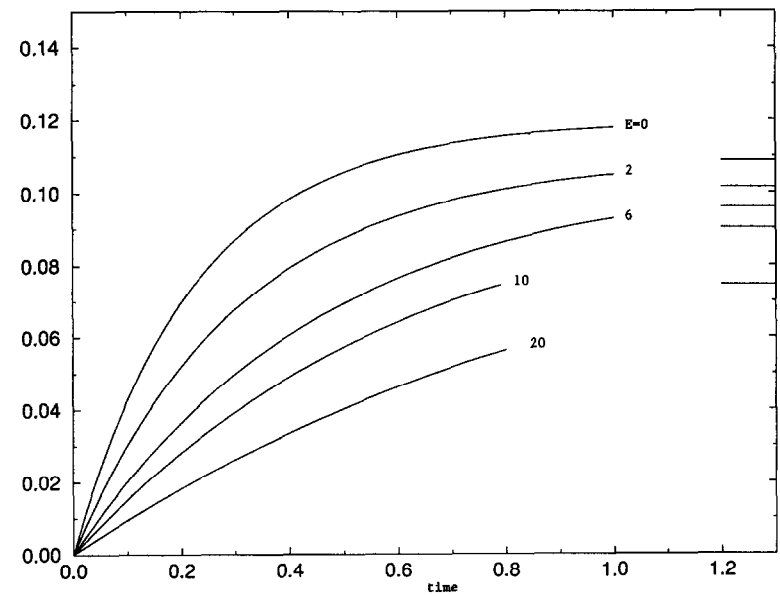

(a)

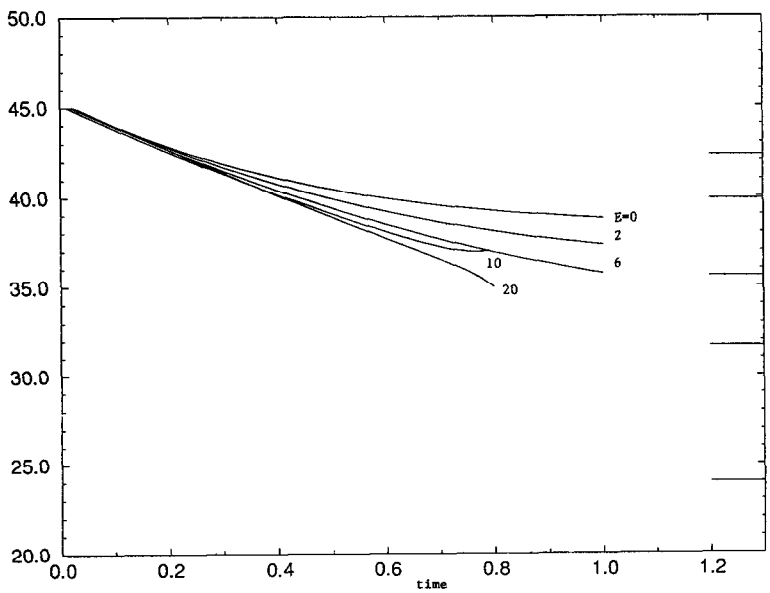

(b)

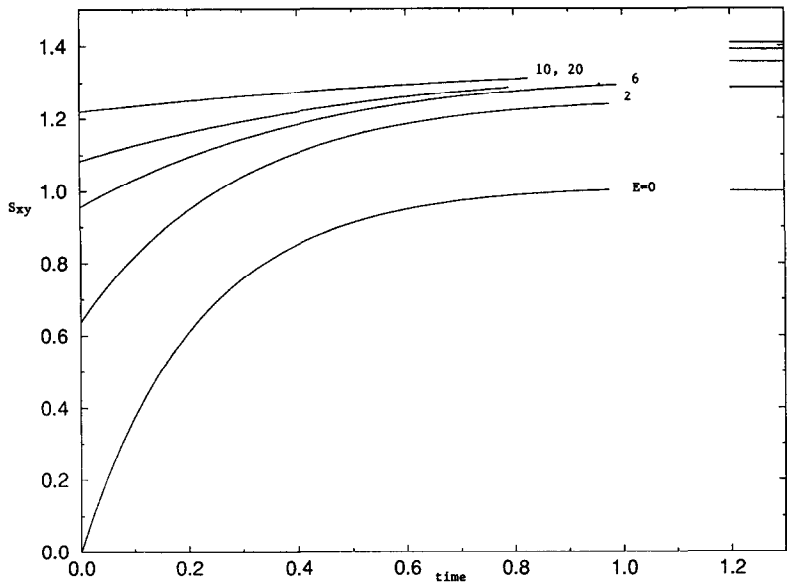

(c)

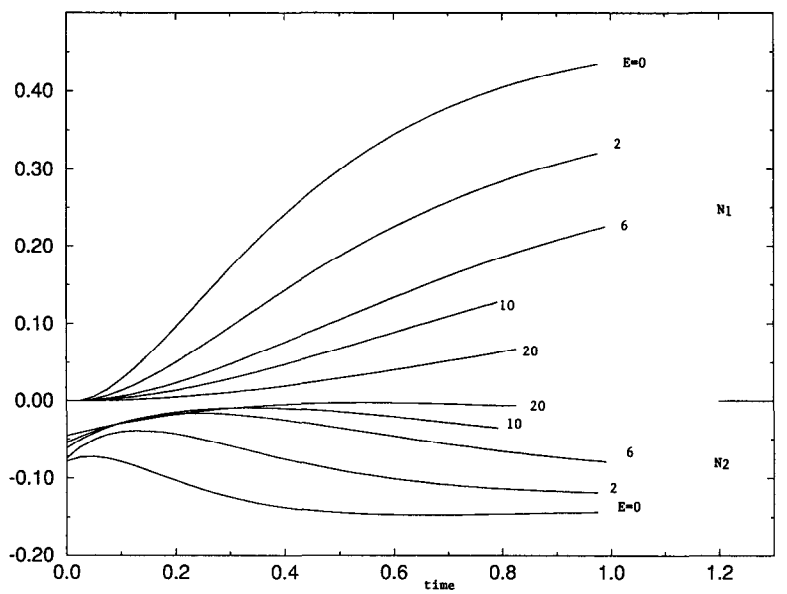

(d)

Fig. 2. Features of the evolution of a spherical drop deforming under the action of a simple shearing flow for $\lambda = 1$ and $Ca = 0.10$, at various values of the surface viscosity ratio E. The evolution of (a) drop deformation D; (b) drop inclination θ; (c) reduced shearing component of the particle stress tensor, which is the added effective shear viscosity of a dilute suspension; (d) reduced first and second normal stress differences.

vanishes, for the presence of the drop interface does not affect the flow. For finite values of E, the presence of the interface generates a perturbation flow even when the drop has a spherical shape, and the particle stress tensor has a finite value.

Figure 2(c) shows a monotonic increase of the effective viscosity in all cases, followed by a transition to asymptotic values at large times. Under the adopted non-dimensionalization, the asymptotic value for $E = 0$ is equal to one. The numerical limits are in good agreement with the predictions of Oldroyd [2] for spherical drops, which are represented by the horizontal lines (see Appendix). Clearly, as the surface viscosity is increased, the viscous dissipation in the flow and in the interface becomes higher, and the effective viscosity of a dilute emulsion is increased. In the limit as E tends to infinity, the drop tends to behave like a rigid particle and the reduced effective shear stress tends to the value 10/7 (see Appendix).

In Fig. 2(d) we plot the evolution of the first and second normal stress differences defined in terms of the particle stress tensor as $N_1 = S_{22} - S_{11}$ and $N_2 = S_{22} - S_{33}$. For a suspension of spherical drops, both N_1 and N_2 are equal to zero; finite values are attributed to drop deformation. We observe the N_1 is positive whereas N_2 is negative in all cases, which indicates that a dilute emulsion shows some elastic properties similar to those exhibited to polymeric solutions. Furthermore, the numerical results indicate that the asymptotic values of both N_1 and N_2 decrease by a considerable factor as E is increased. This behaviour is attributable to the corresponding decrease in drop deformation.

As noted in the introduction, Wei et al. [3] proposed deducing the combination $3\kappa + 2\epsilon$ by observing the period of circulation of marker points around the centre-plane of spherical drops. But for $\lambda = 1$, the variation of the orbital time with E is small, about 10%, and, due to numerical error, our results could not reveal the effect of drop deformation with sufficient accuracy. Similar difficulties prevented us from computing the rate of dissipation at the interface with sufficient accuracy, but we found evidence that the dissipation increases from zero at $E = 0$, to nearly 0.3 at $E = 6$, and to nearly 0.4 at $E = 10$. Based on physical grounds, we expect that the dissipation within an interface with infinite surface viscosity will be finite; in the limit of infinite surface viscosity, the particle rotates as a rigid body and the surface rate of deformation tends to vanish, thus cancelling the effect of the large multiplicative constant E.

We consider next a value of the Capillary number at which, in the absence of surface viscosity, the drop continues to deform without ever reaching a steady shape [8]. Physical intuition suggests that increasing the surface viscosity will make the drop behave more like a rigid particle and thus, it will halt the continuous deformation and will allow the drop to

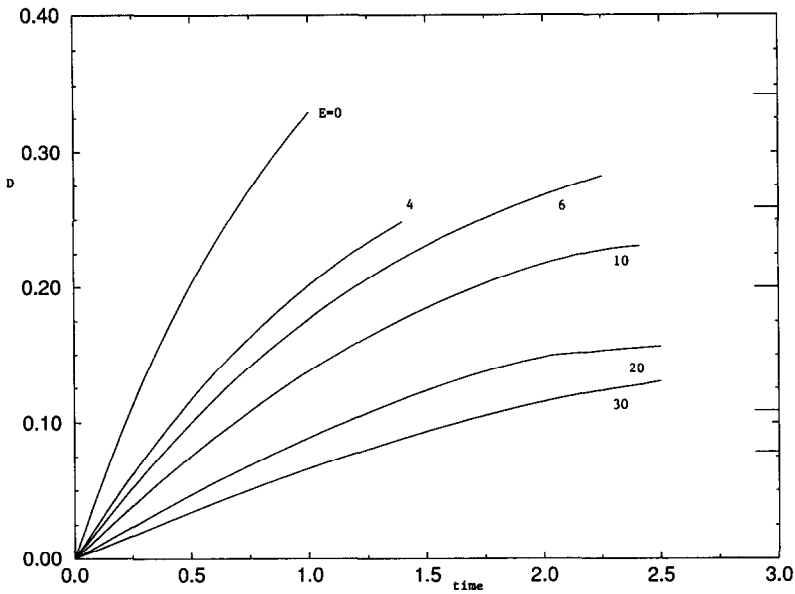

Fig. 3. The deformation D of a spherical drop evolving under the action of a simple shearing flow for $\lambda = 1$ and $Ca = 0.50$, at various values of the surface viscosity ratio E. In the absence of surface viscosity the drop continues to elongate and eventually breaks up. The last portion of the curve for $E = 20$ was computed using a smoothing method to suppress the numerical instability, but this led to a significant distortion of the curve.

reach a stationary shape. This behaviour is also suggested from previous asymptotic analyses. Here we wish to provide further confirmation by direct computation.

In Fig. 3 we plot the history of drop deformation D for several values of E. The numerical results corroborate the notion that there is a critical value of E above which the drop reaches a steady shape at large times. This critical value of E is estimated to be somewhat between 2 and 6. Unfortunately, the 16 by 8 grid did not allow us to compute large deformations and thus assess the critical value of E with better accuracy. In Fig. 3 we also show the predictions of the asymptotic theory of Flumerfelt for slightly deformed drops, shown with straight horizontal lines (see Appendix). The numerical results agree reasonably well with the theoretical predictions for high surface viscosity, but there are noticeable discrepancies at higher deformations where the assumptions of the asymptotic theory cease to be valid.

The last portion of the curve for $E = 20$ in Fig. 3 was obtained by applying numerical smoothing in order to suppress the numerical instabilities. But, we see that this has an important effect on the evolution of the drop and modifies the physics of the motion.

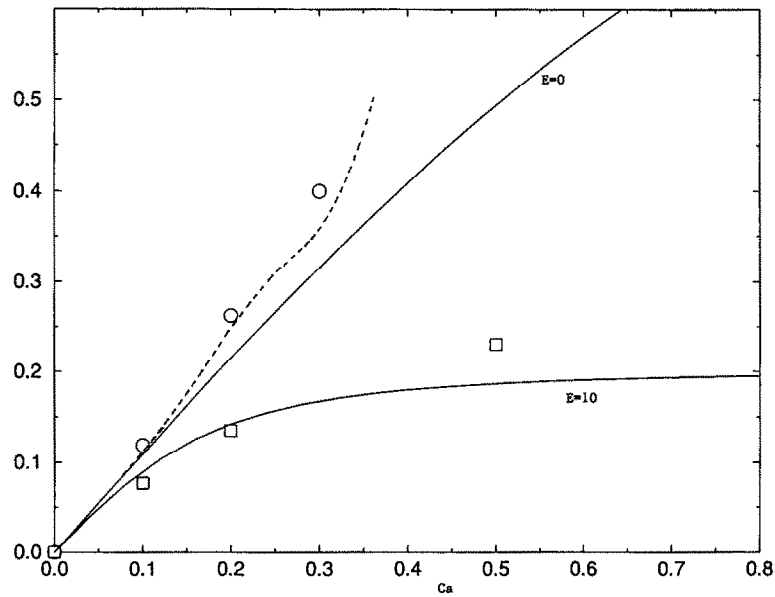

(a)

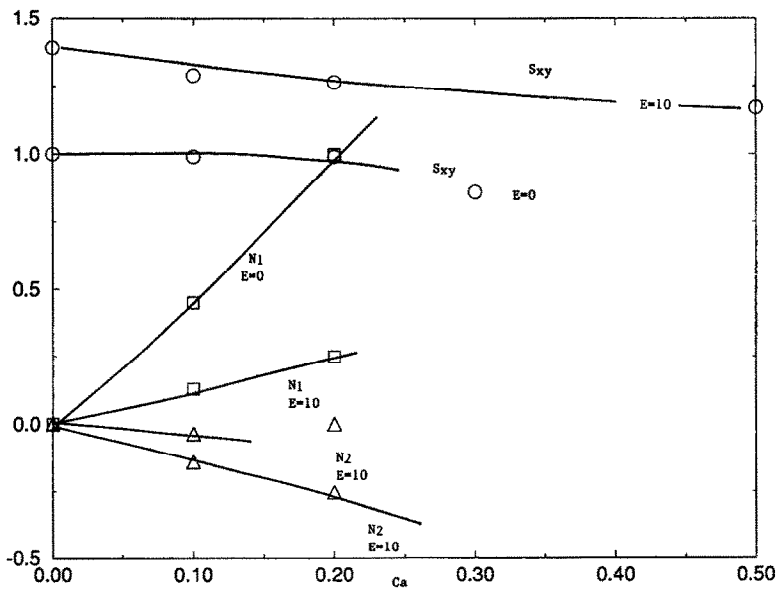

(b)

Fig. 4. (a) The deformation D of stationary deformed drops as a function of Ca for $\lambda = 1$ and $E = 0$ (circles) or $E = 10$ (squares); the dashed line shows the numerical results of Kennedy et al. for $E = 0$ obtained using a different implementation of the boundary integral method [8]. The solid lines show the predictions of the small deformation theory [4]. (b) The reduced shear stress (circles), first normal stress differences (squares), and second normal stress differences (triangles).

To illustrate the effect of surface tension or Capillary number, in Fig. 4(a,b) we plot the drop deformation D, effective shear stress, and normal stress differences, as functions of Ca, for an inviscid interface with $E = 0$ and a viscous interface with $E = 10$. In Fig. 4(a) solid lines show the predictions of the small deformation theory of Flumerfelt [4] (see Appendix), and the symbols indicate our numerical data. The exact curve for $E = 0$ is known to terminate at a value of Ca close to 0.37 beyond which stationary drop shapes cannot be found; the present numerical results are in good agreement with those of previous computations represented by the dashed line [8]. The curve for $E = 10$ appears to extend beyond this inviscid threshold, and it is likely that it is defined at all Capillary numbers. The agreement between the numerical data and the asymptotic predictions is good at small deformations, but the latter underestimates the deformation at large values of Ca.

Figure 4(b) shows that the effective shear stress is a decreasing function of the capillary number, thus suggesting that a dilute suspension behaves like a shear-thinning fluid at both $E = 0$ and 10. The values of the effective viscosity at $Ca = 0$ were computed from the formula of Oldroyd [2] for spherical drops, shown in the Appendix. The magnitude of the normal stress difference is a monotonically increasing function of Ca. An exception appears to be the value of N_2 at $E = 10$, but it is likely that this deviation is due to numerical error. Overall, the results suggest that the presence of finite surface viscosity does not have a profound qualitative influence on the properties of the emulsion. Its main effect is to suppress the interfacial motion and thus make the drop behave like a rigid particle.

Acknowledgement

This research is supported by the National Science Foundation, Grants CTS-9020728 and CTS-9216176.

References

1 J.M. Boussinesq, Ann. Chim. (Phys.), 29 (1913) 349.
2 J.G. Oldroyd, Proc. R. Soc. London Ser. A, 232 (1955) 567.
3 L.-Y. Wei, W. Schmidt and J.C. Slattery, J. Colloid Interface Sci., 48 (1974) 1.
4 R.W. Flumerfelt, J. Colloid Interface Sci., 76 (1980) 330.
5 W.J. Phillips, R.W. Graves and R.W. Flumerfelt, J. Colloid Interface Sci., 76 (1980) 350.
6 D. Barthes-Biesel and H. Sgaier, J. Fluid Mech., 160 (1985) 119.
7 J.C. Slattery, Chem. Eng. Sci., 19 (1964) 379, 453.
8 M. Kennedy, C. Pozrikidis and R. Skalak, Computers Fluids, 23 (1994) 251.
9 L.E. Scriven, Chem. Eng. Sci., 12 (1960) 98.
10 H.A. Stone and L.G. Leal, J. Fluid Mech., 220 (1990) 161.
11 W.J. Milliken, H.A. Stone and L.G. Leal, Phys. Fluids A, 5 (1993) 69.

12 C. Pozrikidis, Boundary Integral and Singularity Methods for Linearized Viscous Flow, Cambridge University Press, Cambridge, 1992.
13 T.W. Secomb and R. Skalak, Q. J. Mech. Appl. Math., 35 (1982) 233.
14 C. Pozrikidis, J. Fluid Mech., 210 (1991) 1.
15 C. Pozrikidis, J. Fluid Mech., 246 (1993) 301.
16 G. I. Taylor, Proc. R. Soc. London Ser. A, 138 (1932) 41.

Appendix

Oldroyd [2] found that the effective shear viscosity of dilute suspension of spherical drops is given by

$$\mu_{\text{Eff}} = \mu\left(1 + c\tfrac{1}{2}\frac{2+5\lambda}{1+\lambda'}\right),$$

where c is the volumetric particle concentration and $\lambda' = \lambda + (2/5)(2\epsilon + 3\kappa)$ is a modified viscosity ratio.

Flumerfelt [4] computed the steady deformation and orientation of a drop in a simple shear flow. In the absence of surfactants and using the present notation, his results show that

$$D = \frac{1}{16(\lambda'+1)}[16 + \lambda'(19 - 9E' + K')]\left[\frac{1}{Ca^2} + \left(\frac{19\lambda'\beta}{20}\right)^2\right]^{-1/2},$$

$$\theta = \frac{\pi}{4} - \tfrac{1}{2}\tan^{-1}\left(\frac{19\lambda'\beta Ca}{20}\right),$$

where

$$E' = \tfrac{4}{5}\frac{E}{\lambda + (2/5)(3K + 2E)}, \qquad K' = \tfrac{3}{2}\frac{K}{E}E'$$

$$\beta = 1 - \tfrac{1}{114}[113K' + 33K' + (K' - 9E')^2].$$